Journal of Structural Geology, Vol. 6, No. 1/2, pp. 5 to 18, 1984
Printed in Great Britain

0191-8141/84 $03.00+0.00
Pergamon Press Ltd.

Strain partitioning in the Helvetic thrust belt of eastern Switzerland from the leading edge to the internal zone

RICHARD H. GROSHONG, JR.

Department of Geology, University of Alabama, University, AL 35486, U.S.A.

O. ADRIAN PFIFFNER

Institut de Géologie, Université de Neuchâtel, CH-2000 Neuchâtel, Switzerland

and

LAUREL R. PRINGLE

Department of Geological and Geophysical Sciences, Princeton University, Princeton, NJ 08544, U.S.A.

(*Accepted in revised form* 28 *June* 1983)

Abstract—The strain and strain partitioning in the Helvetic thrust belt are analysed in order to determine their variation across the belt from the external, thin-skinned portion to the internal, thick-skinned portion, and in order to begin the detailed mechanical analysis of the entire fold-and-thrust belt. Coarse-grained limestones of Jurassic and Cretaceous age were chosen for analysis because they can be traced from the external to the internal zones. The strain within a bed is partitioned into three components: transgranular (pressure solution, microfaults, veins), twinning, granular and intragranular, exclusive of twinning (crystal-plasticity, associated with recrystallization). Transgranular strain was very important in the early history of the Helvetic nappes giving way to twinning at a later stage under tectonic burial. Twinning strain was early in the Infrahelvetic complex, giving way to intracrystalline deformation at the later stage of burial. The transition from transgranular- to intragranular-dominated strain occurred at a vitrinite reflectance value of 3.5%, significantly below the greenschist grade of metamorphism. In a large-scale fold at the leading edge of the Helvetic nappes, transgranular strains were associated with the buckling stage of the fold and twinning occurred during fold-tightening. In more internal parts of the Helvetic nappes twinning strains are also late with regard to transgranular strains, but here their pattern corresponds to the regional finite strain pattern. In the internal zone, the Infrahelvetic complex, twinning seems to have been an early event and records an initial layer-parallel shortening, followed by regional internal deformation with intragranular strains.

INTRODUCTION

THE HELVETIC zone in eastern Switzerland provides the opportunity to follow rocks of the same lithology from very low metamorphic grade, thin-skinned deformation to epizonal grade, thick-skinned deformation in an area that underwent polyphase deformation. One purpose of this research is to identify the deformation mechanisms and how they do or do not change across the belt, as well as to determine any variability in the total strain across the belt. It is also possible to establish the relative succession of individual deformation mechanisms, to bring these mechanisms into the context of the large-scale deformation, and to provide a data set for strain and strain partitioning across the belt that can be used for comparison along-strike in the Helvetic zone, and to fold-and-thrust belts elsewhere. Another purpose of this research is to begin the detailed mechanical analysis of an entire fold-and-thrust belt based upon microtectonic data from throughout the belt. Particular emphasis is put on the twinning mechanism in calcite because suitable coarse-grained rocks are available, and the twin strain-gauge technique gives both a qualitative and quantitative description of the strain. The twinning strains are interpreted in terms of the mechanics of large-scale folds and thrusts and position within the thrust belt. We also relate the twinning to the large finite strains observed in deformed rocks containing strain markers (Pfiffner 1980, 1981).

LOCATION AND GEOLOGIC SETTING

The Helvetic zone of eastern Switzerland (Fig. 1) is a classic area of basement/cover tectonics. Within this zone the Glarus thrust, which has a displacement of up to 40 km, separates the Helvetic nappes in the hanging-wall from the Infrahelvetic complex in the footwall (Fig. 2). The Infrahelvetic complex is a thick-skinned fold-and-thrust belt which seems to have formed under hori-

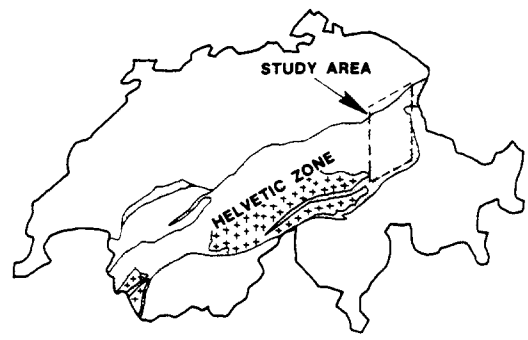

Fig. 1. Map of Switzerland showing the study area in the eastern Helvetic zone. The cross pattern within the Helvetic zone represents the exposed basement massifs.

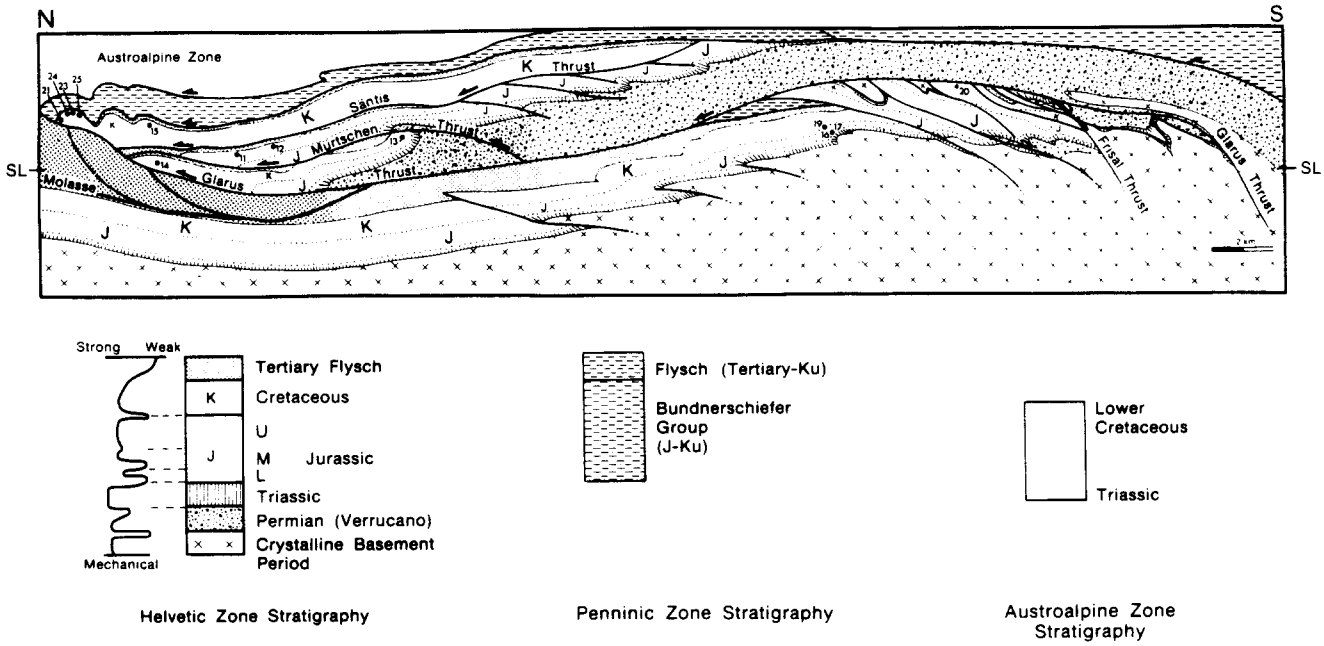

Fig. 2. Synoptic cross-section of the eastern Helvetic zone.

zontal compression and, notably, not by gravity gliding (Milnes & Pfiffner 1980). The Säntis thrust separates the Helvetic nappes into a Lower and Upper Glarus nappe complex (Pfiffner 1980); it represents an upper and lower detachment for these units, respectively, and the maximum displacement is of the order of 10 km. The structural evolution (Milnes & Pfiffner 1977, 1980, Pfiffner 1977, 1978, Schmid 1975, Trümpy 1969) began with a first (Pizol) phase of tectonic burial by higher units, followed by an intricate internal deformation (Cavistrau and Calanda phases), which formed the fold-and-thrust structures and cleavage in the deeper parts. The degree of metamorphism increases from lower metagenic in the frontal parts to epimetamorphic in the internal parts (Fig. 3). A metamorphic event post-dates this internal deformation, because isolines cross-cut the internal structures and chloritoid grew across this cleavage (Pfiffner 1982). Movement along the Glarus overthrust continued after this metamorphic event and produced the local inverse metamorphic zonation. This movement can be correlated with the Ruchi phase crenulation cleavage, which post-dates growth of chloritoid to the largest degree. The latest phase, vertical uplift, is still active today (up to 2 mm/year).

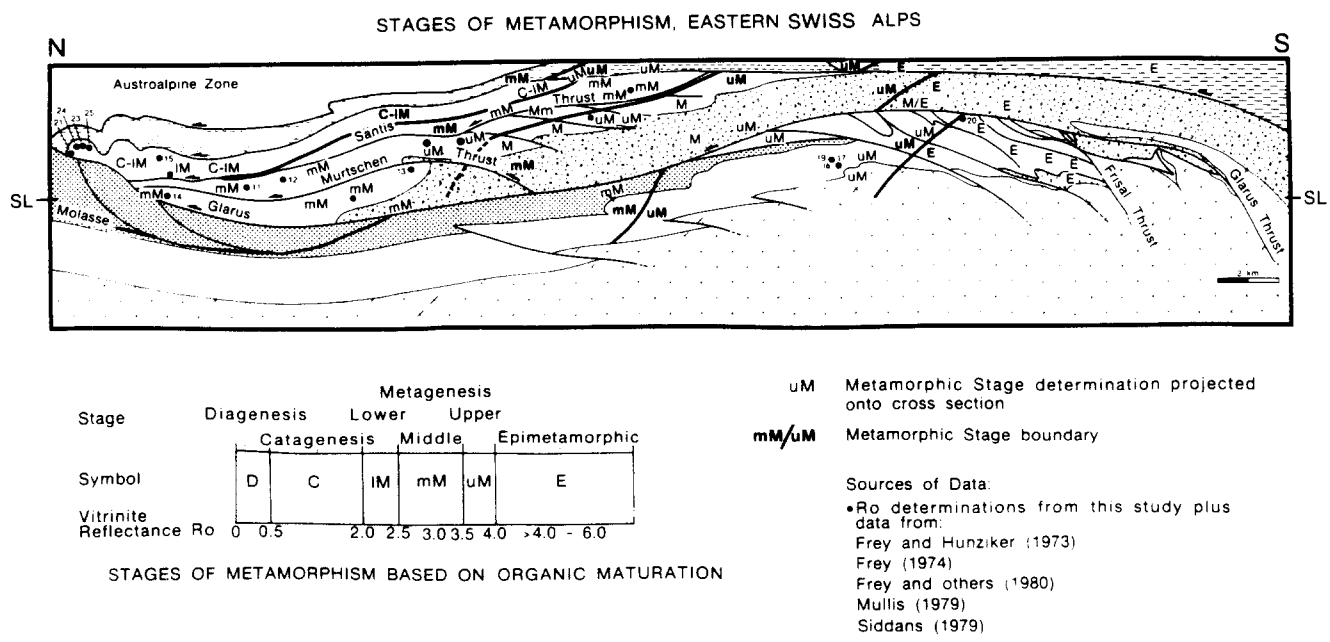

Fig. 3. Stages of metamorphism. Data from within the study area are projected onto the synoptic cross-section shown in Fig. 2.

The basement rocks of the Aar massif consist of polymetamorphic gneisses and metasediments intruded by Variscan granitoids and locally capped by a volcanoclastic series. The cover rocks range from Upper Palaeozoic to Tertiary in age. Mechanically strong members (Fig. 2) include Permian conglomerates, Triassic dolomites, various thick limestones of late Jurassic and Cretaceous age and Tertiary sandstones that are interbedded with various shaly and marly horizons which lead to décollement structures (e.g. the Säntis thrust follows a lowermost Cretaceous shale). Within the Helvetic nappes, the youngest sediments are of Upper Eocene age, whereas in the originally more external Infrahelvetic complex sedimentation continued into the early Oligocene. For this study coarse-grained limestones from the Lower Cretaceous Schrattenkalk-formation were chosen wherever possible (samples 80-14 and 25 are from the lower Cretaceous Oehrli, 80-19 from the Betlis limestone, 80-16 from the Blegi oolite and samples 80-17 and 19 from Middle Jurassic crinoidal and oolitic limestones).

METHODOLOGY

Strain partitioning

Strain partitioning is the subdivision of the total strain at some scale into components produced by different deformation mechanisms. Several mechanisms may be active simultaneously and, as strain increases or as environmental conditions change, certain mechanisms may cease to function and others become prominent. Different mechanisms may measure different components of the same strain, for example, solution cleavage indicating the shortening and mineral fibres indicating the corresponding extension (Mitra 1976), or the different mechanisms may measure completely different episodes of deformation. Thus, in order to interpret the meaning of strain measurements, it is important to determine how the total strain is partitioned between the different deformation mechanisms, and the sequence of events in which these mechanisms were active.

The scale of strain partitioning of interest here is that of the bed. From this perspective the deformation mechanisms of interest include such features as stylolites, bedding-bounded faults and crystal-plastic deformation. In contrast and on a larger scale, the bulk strain in a fold-and-thrust belt might be described in terms of the partitioning between folds and thrusts. Consideration of the strain partitioning is implicit in the work of many researchers and it has been treated explicitly by Nissen (1964), Nickelsen (1966), Arthaud & Mattauer (1969), Groshong (1975), Mitra (1976, 1979), Engelder (1979a, b), Engelder & Geiser (1980), Pfiffner (1980) and Borradaile (1981). Each investigator developed descriptive subdivisions of partitioning based upon his purpose and his particular study area. For our purposes the tripartite subdivision shown in Fig. 4 is convenient. The object is to describe the deformation-induced

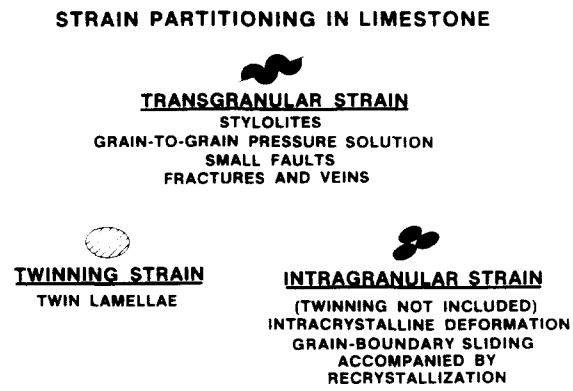

Fig. 4. Strain partitioning in coarse-grained limestones.

changes in a clastic limestone as the strain increases and as the environmental conditions change. The focus is therefore on the original sedimentary grain. Sedimentary grains may be single crystals (e.g. a crinoid stem plate) or a composite of many crystals (e.g. an ooid or a pellet). Matrix or void space is considered separately. However, a single crystal of void fill or cement is treated as a grain. The transgranular strain component cuts grains without deforming them internally. The intragranular strain component represents permanent internal distortion of the grain (crystal-plasticity) and may be accompanied by recrystallization. Even though twinning is intragranular, it is singled out because it is a principal indicator of the small intragranular strains that occur under low temperature and pressure conditions where most other intragranular mechanisms are either inoperative or negligible in importance.

The significance of grain-boundary sliding has recently been discussed by Borradaile (1981). Significant deformation by sliding between sedimentary grains requires that they be uncemented and that either the effective stress be very low to allow for dilation (the independent particulate flow of Borradaile 1981), or that the temperature be high (superplastic flow). The strain partitioning categories shown in Fig. 4 are for cemented rocks or for higher effective stress deformation, and hence grain-boundary sliding is included with crystal-plasticity in intragranular deformation (although it would better be termed intergranular deformation).

Twinning strain

Strain in the limestone aggregate is measured using the least-squares strain-gauge technique on the twinned calcite. The derivation of the method has been described by Groshong (1972, 1974) and will not be repeated here. The basic concept is analogous to that of an engineering strain gauge: a number of gauges that record shear-strain are scattered throughout the rock in a variety of orientations. Here, however, the gauges are part of the rock, rather than being glued on or cast within it. The untwinned crystal is the gauge in its undeformed state; the twinned crystal is the deformed gauge. Both natural and experimental deformation under suitable conditions produce multiple lamellar twins. Numerous thin sections of untwinned limestones, including some from the Jura

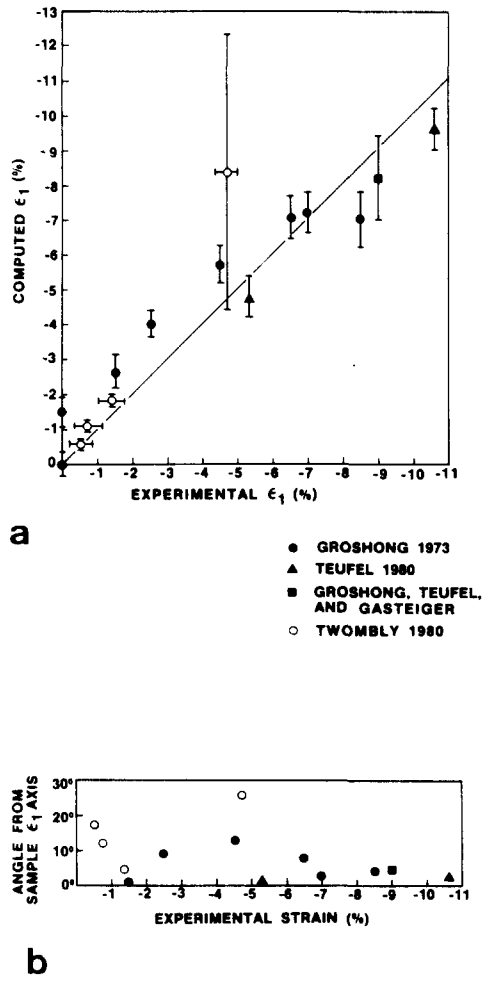

Fig. 5. Experimental test of the calcite strain-gauge technique (from Groshong *et al.* in press). (a) Experimental versus computed compressive strain magnitude. For perfect agreement the points would fall on the straight line. (b) Angular difference between measured and experimental maximum principal compressive strain axis versus magnitude of experimental strain. There is no correlation between angle difference and strain magnitude.

Mountains, demonstrate that lamellar twins do not normally originate by organic or diagenetic growth processes, or from the thin-sectioning process. Under room temperature experimental conditions, the twins are relatively thin, rarely exceeding 5 μm in width, sharply defined and planar (Groshong 1974, Friedman *et al.* 1976). At experimental temperatures above about 300°C the twins are wide, fewer in number and tend to bow outward in the centre (Heard 1963, Schmid *et al.* 1980).

The major requirement that must be fulfilled for the twin strains to correctly measure the strain of the aggregate is that the strain be relatively constant from grain to grain. This hypothesis was shown to provide the best fit to experimental data on Yule marble by Griggs & Miller (1951) and Handin & Griggs (1951). In room-temperature experiments the strain-gauge technique has proved to provide an accurate measure of the total strain (Fig. 5), thus confirming the validity of the assumptions and the calculation technique. Even though the twinning measures the strain, it must be noted that twinning is not the only active intragranular deformation mechanism. Translation glide and grain-boundary adjustments must also occur for the aggregate to retain its continuity (Groshong 1972) and to comply with the von Mises requirement of five independent slip systems.

The probable error of a twin strain computation can be judged from the computed least-squares error. The value of the error on the normal strains in the x and y thin-section coordinate directions are averaged and called the nominal error for the whole strain tensor. This is approximately a one-standard-deviation error. It can be seen in Fig. 5 that the nominal error, so defined, generally provides a good estimate of the actual error. Experiments with multiple thin sections have shown that measurements on 25 grains from two perpendicular thin sections produce results in which the precision is comparable to the accuracy based upon the computed errors (Groshong *et al.* in press). That approach is followed here.

The size of the deviations and the percentage of negative expected values give other parameters with which to judge the accuracy of the result. Once the twins are used to compute a strain tensor for the aggregate, that result is used to compute the expected value of the strain for each twin set, based upon its orientation. The deviation is the difference in magnitude between the measured and computed twin strain. Experience with experimental data sets indicates that deleting the 20% largest deviations improves the result, presumably by eliminating the worst measurement errors and part of any component of inhomogeneous strain. The sense of shear of a twin set can only have one orientation with respect to the crystallography: by the tensor sign convention this sense of shear is positive. A twin for which the expected value of the shear strain is negative has the wrong orientation to be twinned, given the computed strain tensor. A few negative-expected values might be anticipated for grains that have rotated slightly or for which the orientation was not measured sufficiently accurately. A large number of negative-expected values imply very inhomogeneous strain, rotational strain or multiple noncoaxial strain. Negative-expected values in the range of 10–20% are common in most field examples. Negative-expected values over 40% imply very inhomogeneous or multiple deformation. A multiple deformation can be sorted, under favourable circumstances, into its different components (Teufel 1980).

Vitrinite reflectance

Vitrinite is formed during diagenesis from the lignin and cellulose of plant cell walls and is a natural component of coals. Upon heating, the aromatic lamellae of vitrinite become more ordered, resulting in a systematic increase in reflectivity of incident light (Dow & O'Connor 1982). The reflectivity also becomes increasingly birefringent as metamorphism increases. The commonly reported reflectivity value, *Ro*, is an average of random measurements made under high magnification, not the consistent measurement of minimum or maximum reflective values. The increase of reflectance of vitrinite is essentially irreversible and is a function of tempera-

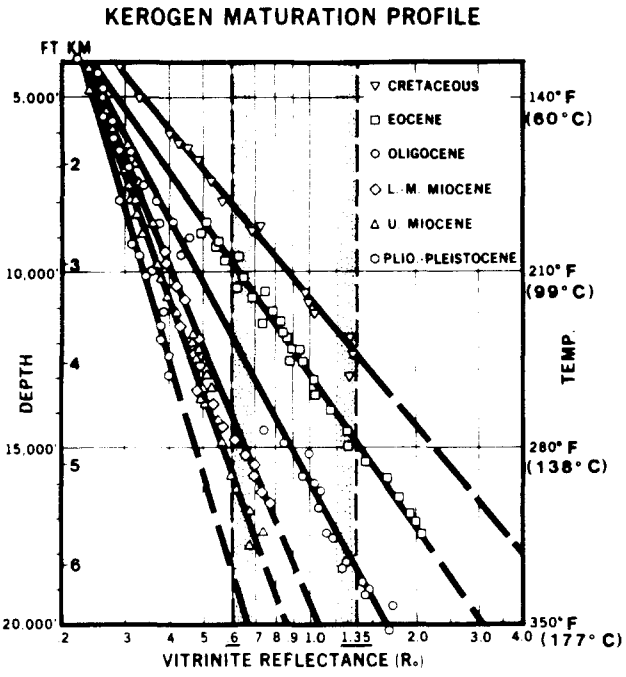

Fig. 6. Composite vitrinite reflectance profiles for two wells in each producing trend of the Gulf of Mexico (Dow 1978). All wells have geothermal gradients close to 25°C/km.

ture, not pressure (Bostick 1974, Hood & Castaño 1974). Other organic indicators such as spore colouration or coal rank also change with temperature and have been correlated to low-temperature mineralogic zones as well (Kübler *et al.* 1979).

The metamorphic stage scale used here (Fig. 3) follows that presented by Tissot & Welte (1978). Diagenesis spans the *Ro* range of 0 to 0.5%. Catagenesis spans the *Ro* range of 0.5–2.0%. This is the range in which liquid petroleum, wet gas and thermal methane are produced. Metagenesis covers the *Ro* range 2.0–4%. This range approximately coincides with what has been called anchimetamorphic (Kübler *et al.* 1979). Above a reflectance of 4.0% the rock is in the epimetamorphic or greenschist facies.

The vitrinite reflectance technique provides important subdivisions of the metamorphic scale below the greenschist grade. The stages of catagenesis and metagenesis have themselves been subdivided in this study to yield more refined units. The measurements, and hence the scale, are reproducible and will work in most detrital rock types that contain some vitrinic organic debris.

The time spent at a given temperature determines the value of *Ro*. This is readily seen from the results of sedimentary sequences found in areas that have constant geothermal gradient but different rates of deposition (Fig. 6). For example, as shown in Fig. 6, an Upper Miocene rock buried to a depth of 5.5 km has an *Ro* value of slightly less than 0.7%, representing a short time at maximum temperature. On the other hand, an Eocene rock at the same depth has an *Ro* value of 2.0%, representing a longer time at maximum temperature (about 157°C).

RESULTS

Metamorphism

A number of studies of metamorphism have been carried out in this general area and concentrated on specific lithologies and hence specific methods. A compilation of these works is given in the synoptic profile in Fig. 3. Data by Frey *et al.* (1980) and Siddans (1979) are on illite crystallinities, Mullis (1979) and Frey *et al.* (1980) on fluid inclusions, and Frey *et al.* (1980) on vitrinite reflectance. Also included are unpublished data by Kübler & Pfiffner on illite crystallinity and new data on vitrinite reflectance carried out for this study (M. Bromily 1982, unpublished Cities Service Co. report).

The *Ro* of 2.5% determined from a Cretaceous shale sample in the Säntis area provides a major control point for the depth of burial. Using the geothermal gradient given in Fig. 6 and assuming constant rate of burial, we see that because there are only about 2 km of sedimentary rocks in normal sequence above the sample, the *Ro* should only be about 0.5%. Deposition and subsequent removal of a great thickness of sediment to explain the high value of 2.5% is unlikely. More likely is tectonic burial. For slow burial (the Cretaceous trend of Fig. 6), about 5 km of overburden is required to produce an *Ro* of 2.5%. For faster burial, the more likely possibility, an even greater depth of burial would be required. This argument ignores the effect of changing thermal gradients or the fact that the overriding block was probably warmer than the autochthonous rocks. We conclude only that substantial tectonic burial was required, not the specific amount of burial. Inspection of the synoptic profile in Fig. 3 shows that the isolines of metamorphic grade cross cut the internal (mainly Calanda phase) structures, but that they are offset along the Glarus thrust.

Twinning strain

The three-dimensional twin-strain magnitudes and directions are shown in Fig. 7. The strain magnitudes are in the range of −0.5% to −8.9%. This range of magnitudes is similar to those seen in previous field studies from thin-skinned thrust belts (Groshong 1975, Engelder 1979a, b, Spang & Groshong 1981, Spang *et al.* 1981). The typical orientation of strain axes in these previous studies is for the maximum compressive strain axis to plunge in the direction of bedding dip, often at a slightly lower angle than the dip and for the maximum extension axis to be either perpendicular to bedding or parallel to strike. This pattern is seen in the Infrahelvetic samples 80-17 and 80-19 as well as in the Glarus nappe complex samples 80-13 and 80-15. The twins in the Infrahelvetic sample 80-16 come from vein fill and pressure shadows and represent an unknown strain increment and fit no obvious orientation pattern. The remaining Glarus nappe complex samples show a consistent and unusual pattern. The maximum compressive strains lie in the N–S plane, independent of the strike of bed-

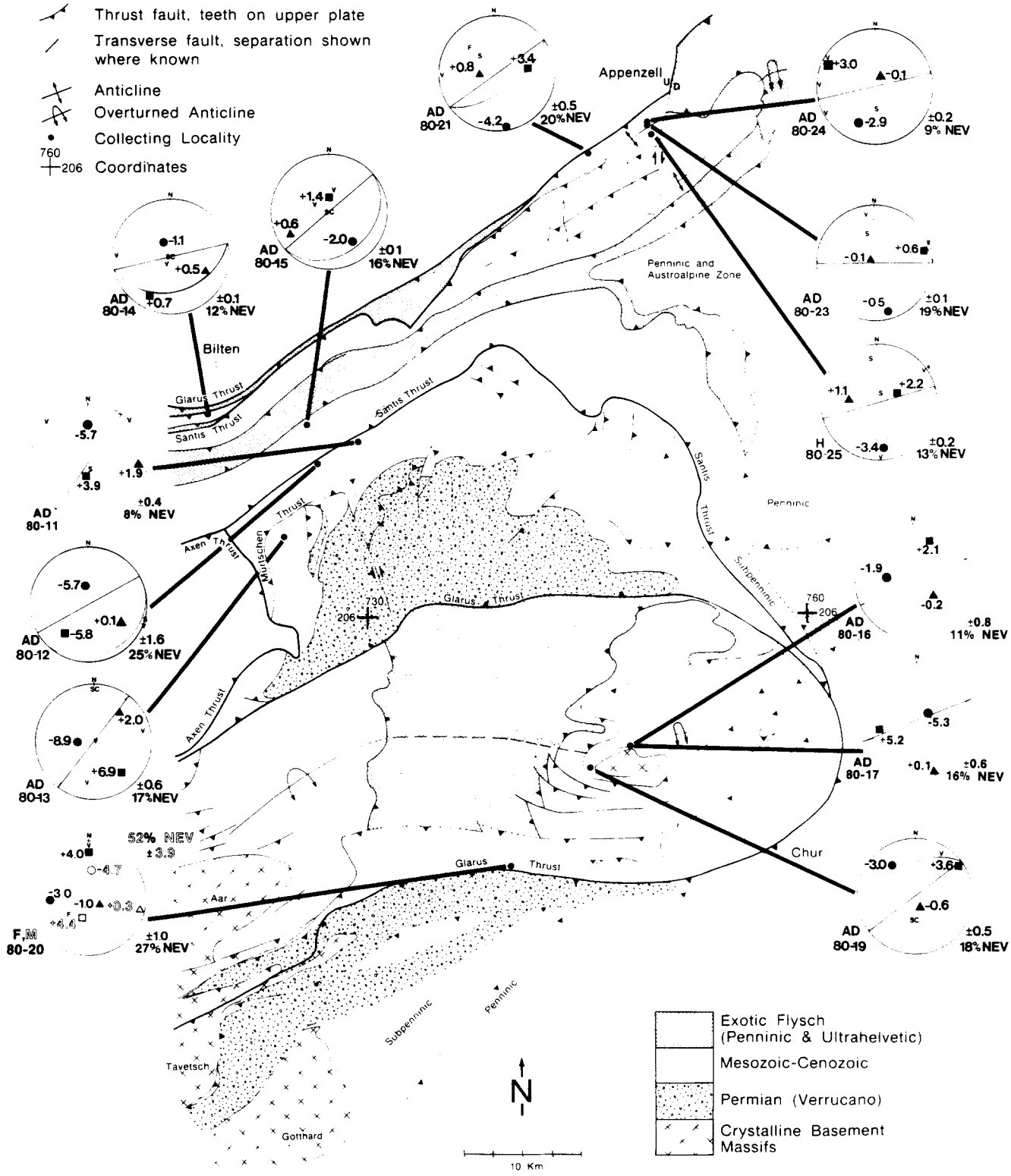

Fig. 7. Horizontal section at a datum 1500 m above sea-level with twin strain data. The stereonets are lower-hemisphere equal-angle projections. The solid great circles give the orientation of bedding (where known). Bedding in samples 16, 17 and 21 is overturned. All strain results are given in % and are computed less the 20% largest deviations; shortening is negative. [(■), maximum extension; ▲, intermediate; ●, maximum shortening axis]; AD, all data used in calculation; H, only host data used in calculation (twins in veins give significantly different results); F, data from fossils alone; M, data from matrix alone. The ± value is the computed nominal error for the strains; %NEV is the percent negative expected values remaining after the computation. V, pole to vein; S, pole to stylolite seam; SC, axis of stylolite columns; F, pole to fault plane; o, pole to cleavage.

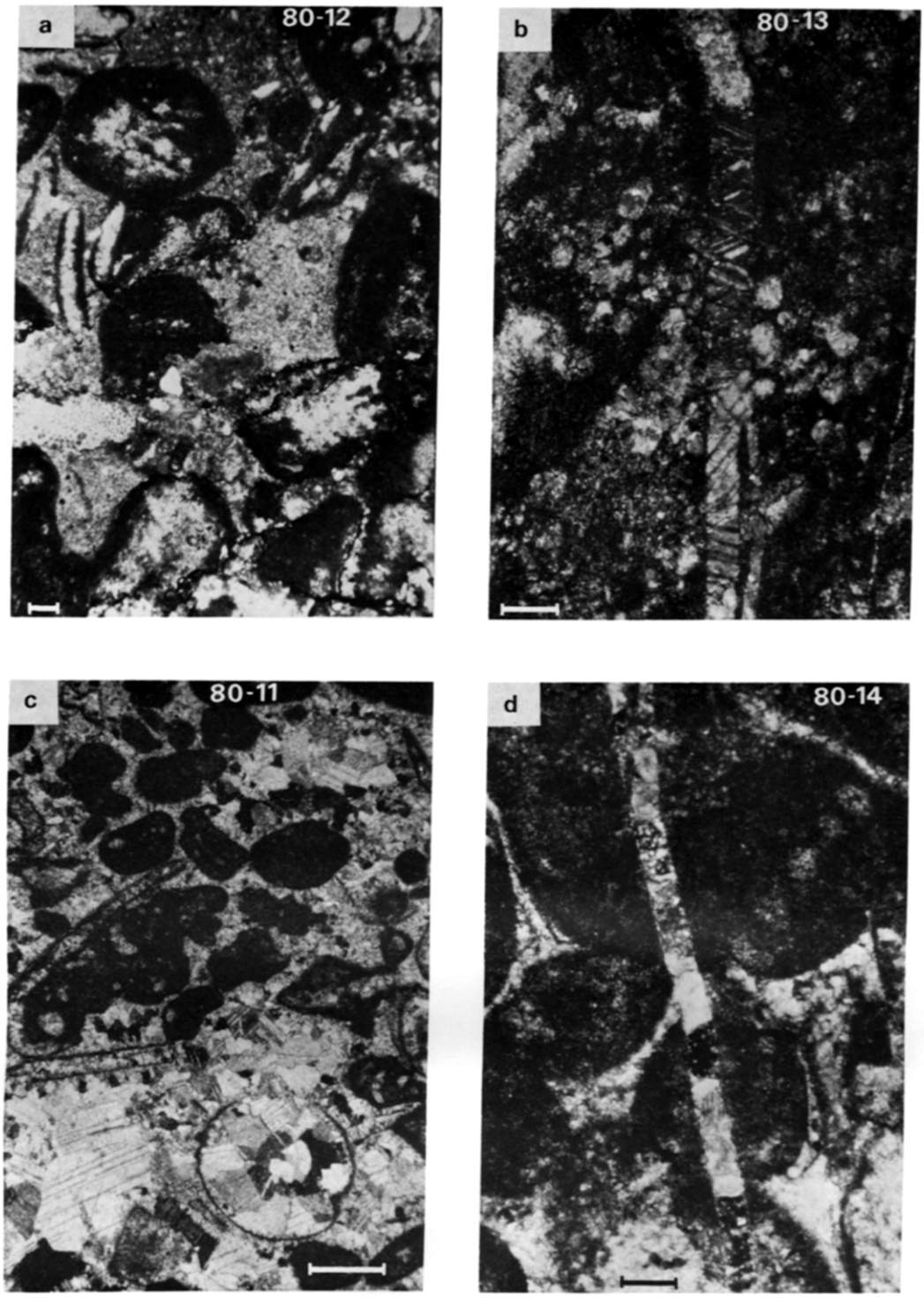

Fig. 8. Thin section photomicrographs of microstructures. Crossed polarizer. Scale-bars are 100 μm, except for (c) and (e) where they are 1 mm. (a) Stylolites. (b) Twinned vein. (c) Twinned spar. (d) Untwinned vein.
(*continued overleaf*)

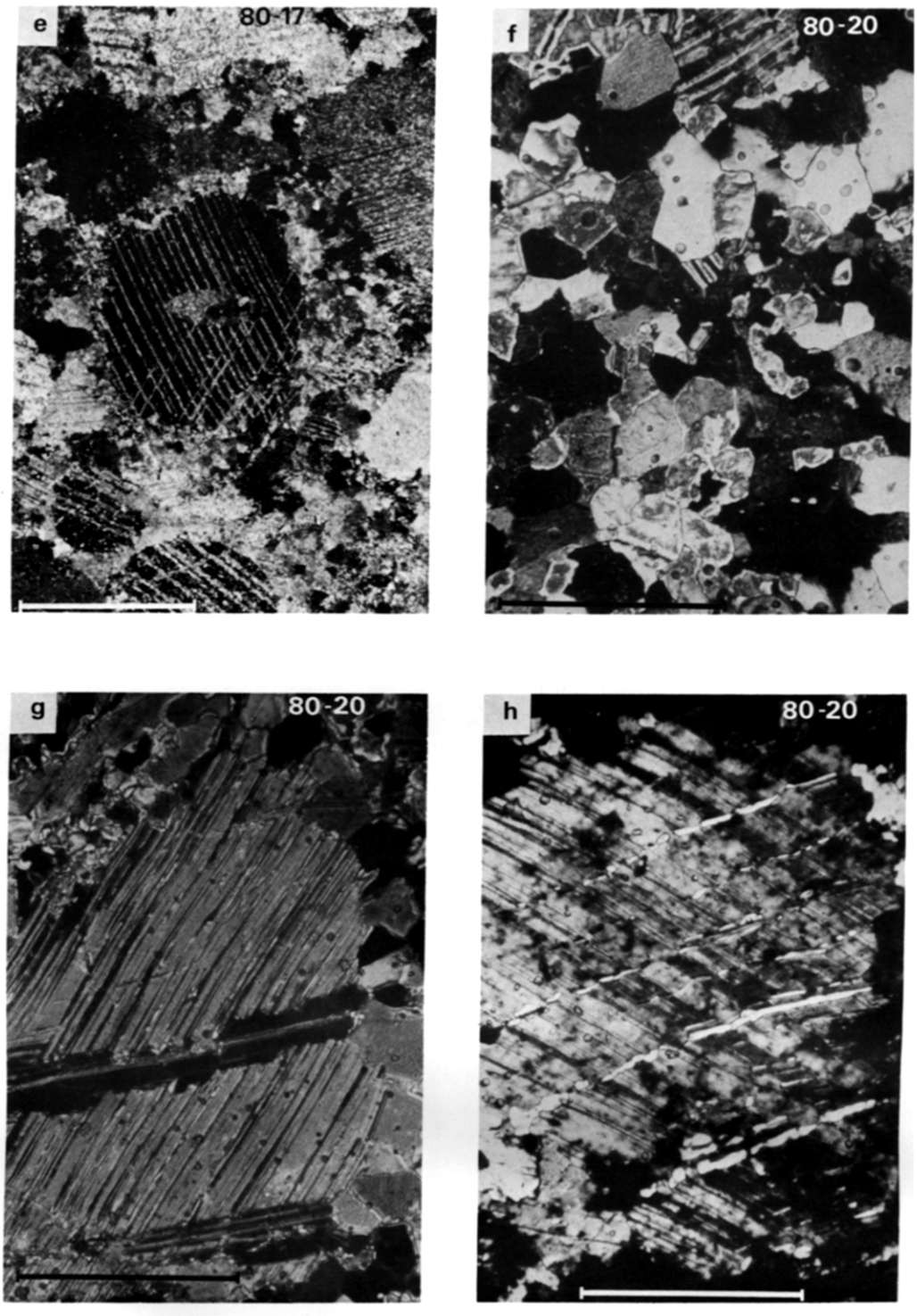

Fig. 8 (*cont.*) (e) Recrystallization leading to serrate outer boundary of crinoid stem. (f) Recrystallization of micritic ooze leading to straight grain boundaries and polygonal grain shapes. (g) Twin-boundary migration causing irregular shape of twin lamellae. (h) Twin-boundary migration transformed former twin lamellae into strings of 'neoblasts'.

ding. The plunges are gently south in the Säntis anticline of the Upper Glarus complex (80-21, 23, 24, 25) and moderately to steeply north plunging in the Lower Glarus complex (80-11, 12, 14). Maximum extension axes tend to be E–W in the Säntis anticline but in the N–S plane in the Lower Glarus complex. Bedding is not definable in sample 80-20 from just below the Glarus thrust, but the coherent strain in the fossils shows the maximum extension strain axis to be N–S and nearly horizontal. A mechanical interpretation of these data will be given after the microstructures are described.

Microstructures

The limestones analysed contain pellets, fossils, some non-carbonate detrital grains and crinoid single crystals. Some samples have a microcrystalline ooze matrix whereas in others the pores are filled with sparry cement.

In the *frontal parts*, the northern edge of the Upper Glarus nappe complex, tectonic stylolites (Fig. 8a) indicate pressure solution and veins (Fig. 8b) indicate fracturing. These veins cut or are cut by stylolites, indicating that these mechanisms were active more or less simultaneously. The veins separate detrital grains and crinoid single crystals into fragments and extend into the adjacent rock and thus seem to be 'unstable cracks'. Vein filling is generally twinned (Fig. 8b) just like the sparry cement, and the fact that the strain ellipsoids for both types of grains in all but one sample are very similar in magnitude and orientation clearly indicates that these veins formed prior to twinning. Untwinned vein filling, on the other hand, occurs in samples taken from near faults (Fig. 8d) and indicates that those veins formed after twinning. Twin lamellae in this frontal part are thin and straight, and the microstructure of the microcrystallize ooze (grain size around 8 μm) is characterized by very complex irregular grain shapes.

In the *intermediate parts*, the Lower Glarus nappe complex, the same basic features are observed except that strains are higher (pellets are somewhat flattened and twin lamellae are thicker) and the grain boundaries of the microcrystalline ooze are simpler although not straight.

In the *internal parts*, the Infrahelvetic complex, stylolites are less common and veins are very rare. Some crinoid single crystals are broken into fragments, but now the fractures are 'stable cracks' and do not extend beyond the crinoid single crystals. The crinoid single crystals begin to be recrystallized at their serrate outer boundaries (Fig. 8e). The microcrystalline matrix and sparry cement are also recrystallized (grain size around 20 μm) and have straight grain boundaries (Fig. 8f). Twin lamellae are thick, often bent, and their occasional irregular boundaries indicate twin boundary migration (Fig. 8g). In some cases the whole of a lamellae is replaced by a string of small new grains (Fig. 8h).

Strain partitioning

The choice of the sampling sites was made in view of the fact that strain partitioning reflects a variety of conditions of deformation. Of primary importance, especially for sedimentary rocks, is lithology (Handin *et al.* 1963) with grain size also having an effect (Hugman & Friedman 1979, Schmid *et al.* 1980). Next in importance are changes in temperature and pressure (grade of metamorphism). Different suites of deformation mechanisms provide one basis for recognizing different structural levels, a subject treated by de Sitter & Zwart (1960), de Sitter (1974) and, in some detail, by Arthaud & Mattauer (1969). Total strain along with metamorphic grade appears to be a primary variable in the textural zonation of Franciscan greywacke (Blake *et al.* 1967). The presence of a reactive pore fluid should enhance pressure solution and stylolite formation; replacement of the pore water by oil appears to inhibit the process (Dunnington 1967). Whether or not the fluid is reactive, high fluid pressures favour extension fracturing and vein formation. The magnitude of differential stress, a variable not assessed in any detail in this paper (see Pfiffner 1982), is related to the strain rate by the constitutive equation and is controlled by the deformation mechanism(s) active under the particular conditions of deformation.

In order to interpret changes in strain partitioning across the Helvetic thrust belt, the lithology is held constant: the coarse-grained limestones of Cretaceous and Jurassic age are encountered all the way from the leading edge to the internal zone. Of the other important parameters, metamorphic grade has been determined and the presence of reactive fluids and fluid pressure effects can be interpreted from the deformation mechanisms. Differential stress/strain rate effects were not independently determined. These latter two parameters might vary systematically across the thrust belt but the most rapid changes are probably from major fault-zones into the country rocks (see Pfiffner 1982 for differential stress, Pfiffner & Ramsay 1982 for strain rate). To examine this aspect of the deformation, two of the samples come from major thrusts, whereas the remainder are from the country rock away from the immediate vicinity of major faults.

A semi-quantitative summary of the strain partitioning is given in Fig. 9. The twin strains given are the averages of the square root of the second invariant of strain, a measure of the total distortion. The transgranular strains have not been measured but are roughly estimated. A fold such as the frontal anticline of the Helvetic nappes (Fig. 10) ought to have compressive strains of the order of 30% (Groshong 1975). The relatively planar Lower Glarus nappe complex might show strains of about the same magnitude to the similar-appearing rocks of the Appalachian Plateau (15%: Engelder & Engelder 1977, Engelder 1979a, b). The intragranular strains have been measured using the distortion of fossils within the limestone and by using pebbles in adjacent units. Sample 80-16 shows grain deformation of 40% shortening and sample 80-20 shows grain deformation of about 75% shortening.

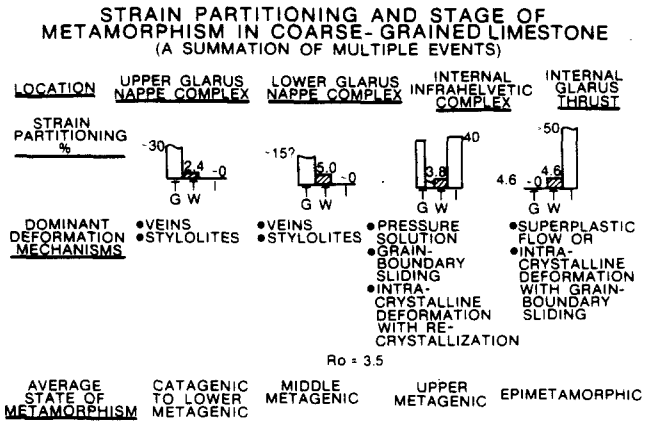

Fig. 9. Strain partitioning and stage of metamorphism in the coarse-grained limestones of the eastern Helvetic zone. The deformation and partitioning record multiple events.

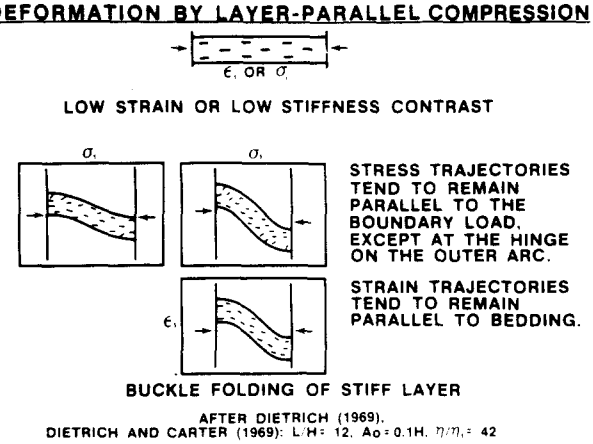

Fig. 11. Compressive stress and strain trajectories in deformation by layer-parallel compression. The buckle component is very small if the strain is low or the stiffness contrast is low, consequently the stress and strain trajectories are nearly parallel (top). The lower diagrams are for stiffness contrasts great enough to allow buckling. L, wavelength; H, thickness; Ao, initial amplitude; η/η_1 = viscosity contrast.

INTERPRETATIONS

Mechanical analysis

Detailed sampling was done across the frontal anticline of the Upper Glarus nappe complex in order to compare it to other field examples of folds and to theoretical models. In Fig. 10 the orientation and magnitude of the twinning shortening strain in the plane of the cross-section is given. The strains are rather uniform in orientation and the pattern resembles the stress orientation expected in a tight buckle fold (Fig. 11). Namely, on the limbs the shortening is at high angle to bedding rather than parallel to it. The high percentage of negative-expected values in sample 80-23 (34% before the largest deviations were removed) indicates a complex or rotational strain history. The compressive strain at this location on the hinge is the smallest value on the fold. Such a history and small strain is expected in the hinge zone of the outer arc in theoretical fold models (Dietrich 1969, Dietrich & Carter 1969, Parrish 1973) because these zones change from layer-parallel shortening to layer-parallel extension. These arguments, together with the fact that twinning post-dates transgranular strains (pressure solution and fracturing) then indicate

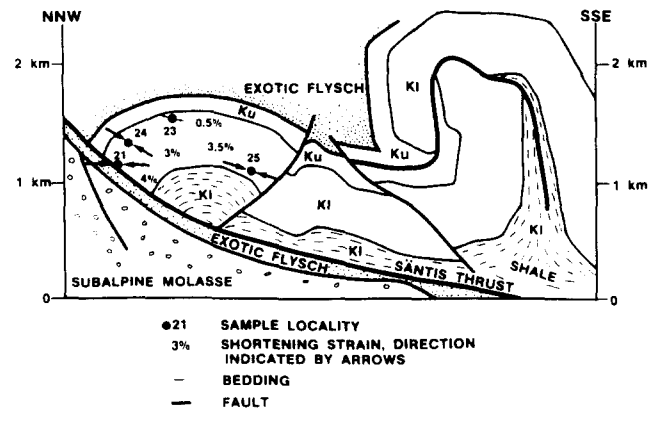

Fig. 10. Detailed cross-section of the frontal portion of the Upper Glarus nappe complex showing maximum compressive strain axes derived from calcite twinning. Kl and Ku, Lower and Upper Cretaceous; dashed pattern, marl/shale. No vertical exaggeration.

that the twinning strains represent a late-stage fold-tightening event. Most of the folding must have occurred by transgranular deformation and was on a NE-trending axis (Fig. 7). The late, fold-tightening twin strain was due to a N–S compression; it was oblique to the fold axis but parallel to the transport direction along the master thrusts (Pfiffner 1981). The layer-parallel shortening of sample 80-15 (Fig. 12) probably occurred during the same late compressional event; the important difference being that at this location the beds were not steeply dipping.

The samples from the Lower Glarus nappe complex have in common that the maximum extension of twinning axes are in the N–S plane, nearly parallel to the regional macroscopically visible stretching lineation (Pfiffner 1981) (Fig. 12). The shortening strain in the plane on the cross-section in Fig. 12, derived from twin measurements, is always perpendicular to the cleavage as seen in adjacent marly or shaly rocks. Twinning post-dates transgranular strain to the largest extent, because the orientation and magnitude of the twin strains in the veins give similar results to the host rock. The twin strain pattern closely resembles the macroscopic finite strain pattern. The latter is characterized by an axial-planar, thrust-parallel cleavage and a regionally constantly oriented stretching lineation parallel to the transport direction along the basal master thrusts. This pattern suggests that the simple shear associated with thrusting is, in part, distributed throughout the region between the Säntis and Glarus thrusts. The regional significance of the early, transgranular strain fraction (veins and stylolites) still needs to be studied.

Samples 80-16, 17, 18, 19 and 20 are from the Infrahelvetic complex. The ambiguity of the strain increment measured renders 80-16 uninterpretable. The other samples, apart from 80-20, show layer-parallel shortening in the plane of the cross-section (Fig. 13). For 80-17 this shortening is nearly perpendicular to cleavage defined by grain-shape flattening. But in 80-19, where this same cleavage is dipping north (parallel to the thrust fault just above the sample site), the twin strain shorten-

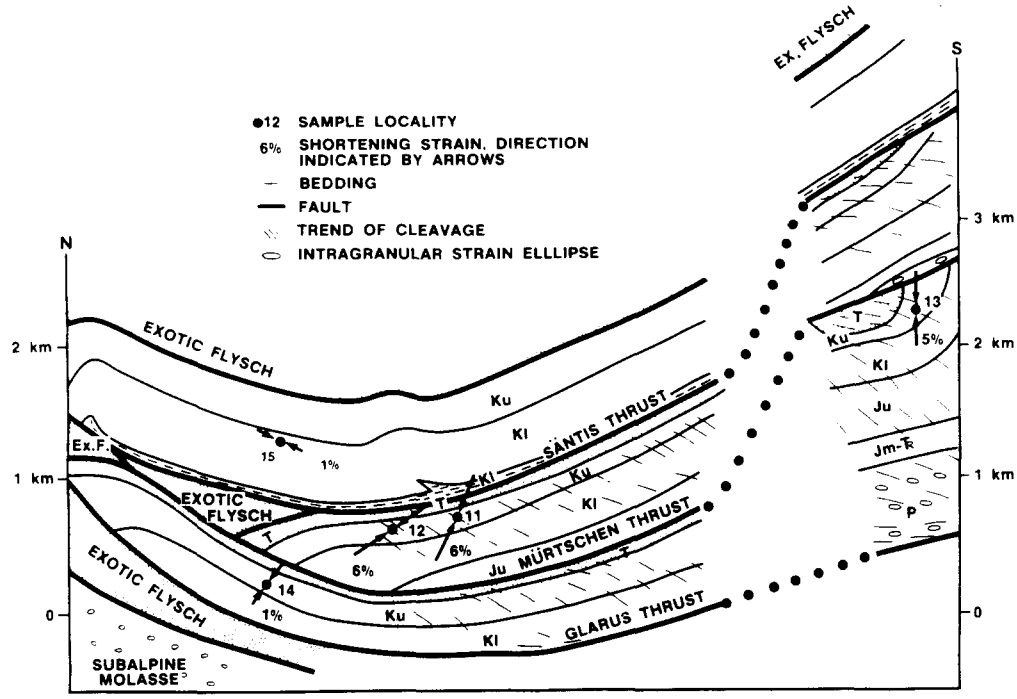

Fig. 12. Detailed cross-section of the Lower Glarus nappe complex showing maximum compressive strain axes derived from calcite twinning, potential cleavage traces and strain ellipses. T, Tertiary; Ku and Kl, Upper and Lower Cretaceous; Ju and Jm, Upper and Middle Jurassic; Tr, Trias; P, Permian. No vertical exaggeration.

ing is roughly parallel to cleavage. This layer-parallel shortening, unlike the one discussed earlier, must be interpreted as an early event within the folding process, particularly because it occurs in the hinge zone of a later, local fold where strain reversals are most probable. In accordance with this there is some twin boundary migration to be seen in these rocks (Fig. 8g) which indicates a shift to other than twinning deformation mechanisms. The crindoids remain relatively circular and hence they have not experienced large strains. The early twin strain indicates a northwesterly compression nearly parallel to bedding. This could represent the regional compression axis at the time of the Helvetic nappes' emplacement, before the late twinning event in the Helvetic nappes.

Sample 80-20 in the Infrahelvetic complex was taken from less than a few metres below the Glarus thrust. The characteristics of the twin strain are different in the few remaining crinoids than in the surrounding finer-grained matrix. The twins from the matrix, computed separately, show 52% negative-expected values, indicating essentially random twin orientations. These high negative-expected values suggest that the twinned grains were subsequently rotated, and accordingly one notes in the adjacent rocks (Pfiffner 1982) a shift to diffusional creep of superplastic flow and twin-boundary migration. The crinoids themselves show 27% negative-expected values. This is an intermediate value, suggesting that a somewhat coherent strain has been measured. The maximum shortening in the cross-section (Fig. 13) is vertical and parallel to the short axes of deformed pebbles in the overlying Permian. Deformed pellets or ooids in sample 80-20 give a shortening strain of about 75% and the axis of maximum elongation plunges steeply to the south. The twins in the intact crinoids thus give essentially the same strain orientations as the pebbles in the overlying Permian, but a different one than the pellets and ooids in the host rock, and the twin strain magnitude is less by one or two orders of magnitude. The twins could measure an early strain that preceded the intracrystalline deformation of the matrix because of the observed twin-boundary migration (Figs. 8g & h), but given the complexities of the strain pattern to be expected in the vicinity of the thrust fault, an interpretation of these results based on one single specimen is left open.

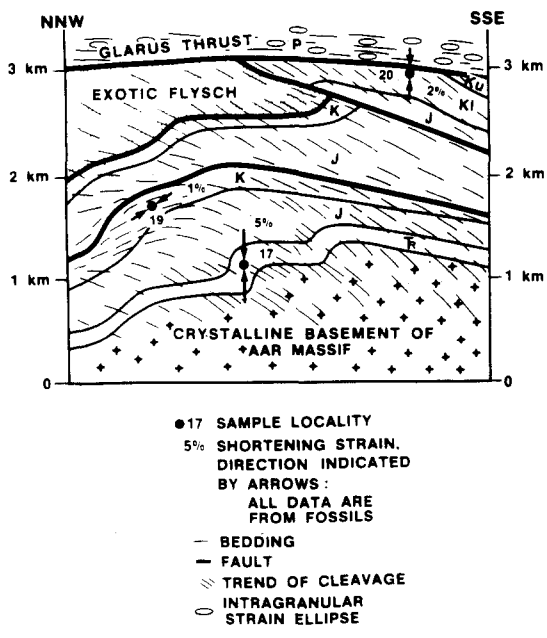

Fig. 13. Detailed cross-section of the internal Infrahelvetic complex showing maximum compressive strain axes derived from calcite twinning; cleavage traces and strain ellipses. Ku and Kl, Upper and Lower Cretaceous; J, Jurassic; Tr, Trias; P, Permian. No vertical exaggeration.

Relative sequences

In the frontal anticline of the Upper Glarus nappe complex, twinning is correlated to a late-stage fold-tightening event and post-dates the transgranular strains which probably accommodated the buckling strains.

The twin-strain fraction seems to be greater in the stack of thrust sheets of the Lower Glarus nappe complex, but again twinning post-dates transgranular strains.

Contrary to this, in the Infrahelvetic complex twinning seems to be an early event of layer-parallel shortening and was followed by intragranular strains due to rising temperatures. Near sample site 80-20 a late twinning event of probably very small magnitude which post-dates the intragranular deformation (Pfiffner 1982), occurs in the matrix of the limestones adjacent to the Glarus thrust.

Within the Helvetic nappes, samples taken from the vicinity of thrust faults (80-13, 14, and 21) contain some untwinned veins and, therefore, indicate late (i.e. post-twinning) fault slip.

Deformation mechanisms and metamorphism

Figure 9 shows the strain partitioning without regard to the history of multiple deformation that has been interpreted in the previous section. Now that the deformation history has been interpreted, the deformation mechanisms can be related to the event in which they occurred and to the probable stage of metamorphism of that event. Figure 14 shows the strain partitioning as it probably occurred in any single event at different stages of metamorphism.

Transgranular strains are important in the Helvetic nappes, in particular in the Upper Glarus nappe complex, that is, in rocks whose metamorphic grade does not exceed the stage of lower metagenesis. The peak of metamorphism post-dates the internal deformation. Twinning here was late and hence occurred at higher temperatures than the transgranular strain, possibly near metagenesis conditions. The same arguments are true for the Lower Glarus nappe complex, where twinning strains are the highest ones encountered and where the metamorphic grade reached middle metagenesis conditions for the sample sites of this study. In the Infrahelvetic complex, high metagenesis and epizonal conditions were reached after the internal deformation and, because twinning was early with regard to the internal deformation, it must have occurred under rising temperatures. Depending on the thermal history, twinning could well have occurred under conditions of lower metagenesis. Intragranular strains, finally, are important in rocks whose metamorphic grade reached higher metagenesis and epizonal conditions. It follows therefore that a major change-over from largely transgranular to intragranular deformation takes place at a vitrinite reflectance value *Ro* of near 3.5 (middle metagenesis, around 270°). Twinning as a deformation mechanism

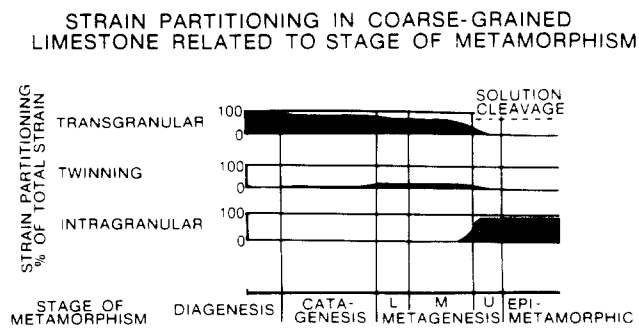

Fig. 14. Strain partitioning in coarse-grained limestones related to stage of metamorphism in the eastern Helvetic zone.

seems to be particularly important on the low-temperature side of this change-over zone.

The deformation of sample 80-20 from the internal portion of the Glarus thrust is quite different from that of sample 80-21, which is from the Glarus–Säntis thrust in its most external position. As described previously, sample 80-20 shows a small relict twin strain and a large superimposed intragranular strain. The major deformation of sample 80-21 is by closely spaced transgranular microfaulting. The original rock fabric between microfaults is generally well preserved and only slightly deformed. As noted in a previous section, the twin strain appears to have been superimposed after this internal deformation and bedding dip were imposed. The initial deformation of 80–21 was probably at diagenetic conditions (Fig. 14) and changed to catagenetic conditions later. The internal Glarus thrust sample retains no record of transgranular deformation. Twinning, the first recorded event, was probably under catagenic or lower to middle metagenic conditions with the principal deformation occurring under upper metagenic to epizonal metamorphic conditions.

OROGENIC EVOLUTION

Combining stratigraphic evidence, structural analysis, the thermal record, and age dating, one arrives at the following orogenic evolutionary sequence.

The first event that the rocks experienced was tectonic burial by emplacement of Penninic nappes whose basal thrusts were folded by subsequent deformations. This first, Pizol, phase must post-date the youngest sediments which are late Eocene in the Helvetic nappes and early Oligocene in the Infrahelvetic complex. It could have been younger in the originally more external Infrahelvetic complex.

Then followed the main internal deformation of the Cavistrau and Calanda phases which includes the development of the Glarus and Säntis master thrusts. Remembering that isolines cross-cut the internal structure now produced, and taking into account the relatively high metamorphic grade in the Infrahelvetic complex (needing considerable overburden) and the low metamorphic grade of the trailing edge of the Helvetic nappes (they must have escaped this overburden), it follows that the internal deformation of the Helvetic

nappes and their emplacement onto the Infrahelvetic complex took place before the internal deformation of the Infrahelvetic complex. The phases defined by structural features are diachronous and indicate a progression of deformation from originally more internal to more external parts within the Helvetic zone.

Subsequent to the internal deformation, followed the Ruchi phase, an episode of additional movement along the Glarus thrust which essentially post-dates the peak of metamorphism and thus led to the local inverse metamorphic zonation (Fig. 3). For the Helvetic nappes it was a phase of passive transport of the internal structure which brought the rocks nearer to the surface (Milnes & Pfiffner 1980). It coincides in time with the formation of the Subalpine Molasse thrust sheets that also show a progression of thrusting from the internal parts toward the foreland. In Fig. 2 the Glarus thrust is shown to splay in the north to form the duplex structure of the Subalpine Molasse thrust sheets. The uppermost possible splay is the Säntis thrust near 80–21 and the late untwinned veins in that sample could therefore be associated with this Ruchi phase. Radiometric dating (K–Ar ages on illites, riebeckite, stilpnomelane and glauconite, Frey *et al.* 1974) yield Oligocene ages in the Helvetic nappes and Miocene ages in the Infrahelvetic complex. These Miocene ages could possibly date the Ruchi phase crenulation cleavage which in turn is associated with slip along the Glarus thrust and the stratigraphic record of the Subalpine Molasse makes Miocene, that is contemporaneous, deformation plausible (Milnes & Pfiffner 1980).

CONCLUSIONS

Strain partitioning within the coarse-grained limestone beds of the Helvetic zone in eastern Switzerland changes as a function of temperature. Deformation at the lowest, diagenetic, temperature appears to be entirely by transgranular mechanisms. Twinning becomes important under catagenic to middle metagenic conditions. The transition to large intragranular strains that cause the rock to look metamorphic occurs at a vitrinite reflectance value of 3.5%, below the greenschist grade boundary. This reflectance value also marks the beginning of basement involvement in the folding.

The Upper Glarus nappe complex was deformed and folded by transgranular mechanisms under low overburden, then deformed by twinning under a greater tectonic overburden. The Lower Glarus nappe complex was also deformed by transgranular mechanisms but did not fold in its frontal part, then it deformed by twinning under the tectonic overburden. The tectonic overburden appears to have been caused by the northward transport of the Penninic and Austroalpine nappes over the Helvetic nappes.

The early twin strain in the Infrahelvetic complex probably reflects a horizontal compression axis that caused the Helvetic nappes to be pushed over the Infrahelvetic complex. The later intragranular strain appears to have occurred after burial by the emplacement of the Helvetic, Penninic and Austroalpine nappes.

Analysis of twinning strain and strain partitioning provides a powerful technique for the quantitative analysis of deformation and deformation history in the Helvetic zone from the external to the internal portions.

Acknowledgements—The support of Cities Service Company where Groshong and Pringle were employed during this research and permission to publish is gratefully acknowledged. Pfiffner received financial support from Schweizerischer Nationalfonds grants nr. 2.859-0.77 and 2.488-0.79. Constructive criticism from Cynthia Scheiner at an early stage of the preparation of this paper and from the reviewers, J. Spang, S. Schmid and M. Casey, was most helpful.

REFERENCES

Arthaud, F. & Mattauer, M. 1969. Les déformations naturelles. Essai d'evaluation des conditions pression température des différents types de déformation. *Spec. No. Rev. Ind. Minér.* 73–81.

Blake, M. C., Jr., Irwin, W. P. & Coleman, R. C. 1967. Upside-down metamorphic zonation, blueschist facies, along a regional thrust in California and Oregon. *Prof. Pap. U.S. geol. Surv.* **57-C**, C1–C9.

Borradaile, G. J. 1981. Particulate flow of rock and the formation of cleavage. *Tectonophysics* **72**, 305–321.

Bostick, N. H. 1974. Phytoclasts as indicators of thermal metamorphism, Franciscan assemblage and Great Valley Sequence (upper Mesozoic), California. *Spec. Pap. geol. Soc. Am.* **153**, 1–17.

Dietrich, J. H. 1969. Origin of cleavage in folded rocks. *Am. J. Sci.* **267**, 155–165.

Dietrich, J. H. & Carter, N. L. 1969. Stress-history of folding. *Am. J. Sci.* **267**, 129–154.

Dow, W. G. 1978. Petroleum source beds on continental slopes and rises. *Bull. Am. Ass. Petrol. Geol.* **62**, 1584–1606.

Dow, W. G. & O'Connor, D. I. 1982. Kerogen maturity and type by reflected light microscopy applied to petroleum exploration. In: *How to Assess Maturation and Paleotemperatures* (edited by Staplin, F. L., *et al.*). Society of Economic Paleontologists and Mineralogists, Short Course No. 7, 133–151.

Dunnington, H. V. 1967. Aspects of diagenesis and shape change in stylolitic limestone reservoirs. *Proc. 7th World Petrol. Cong. Mexico*, **2**, 339–352.

Engelder, T. 1979a. Mechanisms for strain within the Upper Devonian clastic sequence of the Appalachian Plateau, western New York. *Am. J. Sci.* **279**, 527–542.

Engelder, T. 1979b. The nature of deformation within the outer limits of the central Appalachian foreland fold and thrust belt in New York State. *Tectonophysics* **55**, 298–310.

Engelder, T. & Engelder, R. 1977. Fossil distortion and décollement tectonics of the Appalachian Plateau. *Geology* **5**, 457–460.

Engelder, T. & Geiser, P. 1980. On the use of regional joint sets as trajectories of paleostress fields during the development of the Appalachian Plateau, New York. *J. geophys. Res.* **85**, 6319–6341.

Frey, M. 1974. Alpine metamorphism of pelitic and marly rocks of the Central Alps. *Schweiz. Miner. Petrogr. Mitt.* **54**, 489–506.

Frey, M. 1978. Progressive low-grade metamorphism of a black shale formation, Central Swiss Alps, with special reference to pyrophyllite and margarite bearing assemblages. *J. Petrology* **19**, 93–135.

Frey, M., Hunziker, J. C., Roggwiller, P. & Schindler, C. 1973. Progressive niedriggardige Metamorphose glaukonitführender Horizonte in den helvetischen Alpen der Ostschweiz. *Contr. Miner. Petrol.* **39**, 185–218.

Frey, M., Hunziker, J. C., Frank, W., Bocquet, J., Dal Piaz, G. V., Jäger, E. & Niggli, E. 1974. Alpine metamorphism of the Alps: a review. *Schweiz. Miner. Petrogr. Mitt.* **54**, 247–290.

Frey, M., Teichmüller, M., Teichmüller, R., Mullis, J., Künzi, B., Breitschmid, A., Gruner, U. & Schwizer, B. 1980. Very low-grade metamorphism in external parts of the Central Alps: illite crystallinity, coal rank and fluid inclusion data. *Eclog. geol. Helv.* **73**, 173–203.

Friedman, M., Teufel, L. W. & Morse, J. D. 1976. Strain and stress analysis from calcite twin lamellae in experimental buckles and faulted drape-folds. *Phil. Trans. R. Soc.* **A283**, 87–107.

Griggs, D. & Handin, J. 1960. Observations on fracture and a hypothesis of earthquakes. *Mem. geol. Soc. Am.* **79**, 347–364.

Griggs, D. & Miller, W. B. 1951. Deformation of Yule marble—Part I. Compression and extension experiments on dry Yule marble at 10,000 atmospheres confining pressure, room temperature. *Bull. geol. Soc. Am.* **62**, 853–862.

Groshong, R. H., Jr. 1972. Strain calculated from twinning in calcite. *Bull. geol. Soc. Am.* **82**, 2025–2038.

Groshong, R. H., Jr. 1974. Experimental test of least-squares strain gauge calculation using twinned calcite. *Bull. geol. Soc. Am.* **86**, 1855–1864.

Groshong, R. H., Jr. 1975. Strain, fractures, and pressure solution in natural single-layer folds. *Bull. geol. Soc. Am.* **86**, 1363–1376.

Groshong, R. H., Jr., Teufel, L. W. & Gasteiger, C., in press. Precision and accuracy of the calcite strain-gauge technique. *Bull. geol. Soc. Am.*

Handin, J. W. & Griggs, D. 1951. Deformation of Yule marble—Part II. Predicted fabric changes. *Bull. geol. Soc. Am.* **62**, 863–886.

Handin, J., Hager, R. V., Friedman, M. & Feather, J. N. 1963. Experimental deformation of sedimentary rocks under confining pressure: pore pressure tests. *Bull. Am. Ass. Petrol. Geol.* **47**, 717–755.

Heard, H. C. 1963. The effect of large changes in strain rate in the experimental deformation of Yule marble. *J. Geol.* **71**, 162–195.

Hood, A. & Castaño, J. R. 1974. Organic metamorphism: its relationship to petroleum generation and application to studies of authigenic minerals. *United Nations ESCAP, CCP Technical Bulletin* **8**, 85–118.

Hugman, R. H. H., III & Friedman, M. 1979. Effects of texture and composition on mechanical behavior of experimentally deformed carbonate rocks. *Bull. Am. Ass. Petrol. Geol.* **63**, 1478–1489.

Kübler, B., Pittion, J. L., Heroux, Y., Charrollais, J. & Weidmann, M. 1979. Sur le pouvoir réflecteur de la vitrinite dans quelques roches du Jura, de la Molasse et des Nappes préalpines, helvétiques et penniques. *Eclog. geol. Helv.* **72**, 347–373.

Milnes, A. G. & Pfiffner, O. A. 1977. Structural development of the Infrahelvetic complex, eastern Switzerland. *Eclog. geol. Helv.* **70**, 83–95.

Milnes, A. G. & Pfiffner, O. A. 1980. Tectonic evolution of the Central Alps in the cross section St. Gallen–Como. *Eclog. geol. Helv.* **73**, 619–633.

Mitra, S. 1976. A quantitative study of deformation mechanisms and finite strain in quartzites. *Contr. Miner. Petrol.* **59**, 203–226.

Mitra, S. 1979. Deformation at various scales in the South Mountain anticlinorium of the central Appalachians: summary. *Bull. geol. Soc. Am.* **90**, 227–229.

Mullis, J. 1979. The system methane–water as a geologic thermometer and barometer from the external part of the Central Alps. *Bull. Minéral.* **102**, 526–536.

Nickelsen, R. P. 1966. Fossil distortion and penetrative rock deformation in the Appalachian Plateau, Pennsylvania. *J. Geol.* **74**, 924–931.

Nissen, H. U. 1964. Dynamic and kinematic analysis of deformed crinoid stems in a quartz graywacke. *J. Geol.* **72**, 346–360.

Parrish, D. K. 1973. A nonlinear finite element fold model. *Am. J. Sci.* **273**, 318–334.

Pfiffner, O. A. 1977. Tektonische Untersuchungen im Infrahelvetikum der Ostschweiz. *Mitt. Geol. Inst. ETH Univ. Zürich, N.F.* **217**, 1–432.

Pfiffner, O. A. 1978. Der Falten- und Kleindeckenbau im Infrahelvetikum der Ostschweiz. *Eclog. geol. Helv.* **71**, 61–84.

Pfiffner, O. A. 1980. Strain analysis in folds (Infrahelvetic Complex, Central Alps). *Tectonophysics* **61**, 337–362.

Pfiffner, O. A. 1981. Fold-and-thrust tectonics in the Helvetic nappes (E. Switzerland). In: *Thrust and Nappe Tectonics* (edited by McClay, K. R. & Price, N. J.). *Spec. Publs geol. Soc. Lond.* **9**, 319–327.

Pfiffner, O. A. 1982. Deformation mechanisms and flow regimes in limestones from the Helvetic zone of the Swiss Alps. *J. Struct. Geol.* **4**, 429–442.

Pfiffner, O. A. & Ramsay, J. G. 1982. Constraints on geological strain rates: arguments from finite strain states of naturally deformed rocks. *J. geophys. Res.* **87B**, 311–321.

Schmid, S. M. 1975. The Glarus overthrust: field evidence and mechanical model. *Eclog. geol. Helv.* **68**, 247–280.

Schmid, S. M., Paterson, M. S. & Boland, J. N. 1980. High temperature flow and dynamic recrystallization in Carrara marble. *Tectonophysics* **65**, 245–280.

Siddans, A. W. B. 1979. Deformation, metamorphism and texture development in Permian mudstones of the Glarus Alps (eastern Switzerland). *Eclog. geol. Helv.* **72**, 601–621.

de Sitter, L. U. 1964. Variation in tectonic style. *Bull. Can. Petrol. Geol.* **12**, 263–278.

de Sitter, L. U. & Zwart, H. J. 1960. Tectonic development in supra- and infrastructures of a mountain chain. *Proc. 21st Int. Geol. Congr.*, Copenhagen **18**, 248–256.

Spang, J. H. & Groshong, R. H., Jr. 1981. Deformation mechanisms and strain history of a minor fold from the Appalachian Valley and Ridge Province. *Tectonophysics* **72**, 323–342.

Spang, J. H., Wolcott, T. L. & Serra, S. 1981. Strain in the ramp regions of two minor thrusts, southern Canadian Rocky Mountains. *Mon. Am. geophys. Union* **24**, 243–250.

Teufel, L. W. 1980. Strain analysis of experimental superposed deformation using calcite twin lamellae. *Tectonophysics* **65**, 291–309.

Tissot, B. P. & Welte, D. H. 1978. *Petroleum Formation and Occurence*. Springer, New York.

Trümpy, R. 1969. Die helvetischen Decken der Ostschweiz: Versuch einer palinspastischen Korrelation und Ansätze zu einer kinematischen Analyse. *Eclog. geol. Helv.* **62**, 105–142.